

**Effect of different precursors on morphology of CVD Synthesized
MoSe₂**

A PROJECT REPORT
SUBMITTED IN PARTIAL FULFILMENT OF THE REQUIREMENTS FOR
THE
AWARD OF THE DEGREE
OF

MASTER OF SCIENCE
IN
[PHYSICS]

Submitted by

VINAY KUMAR YADAV
(2K19/MSCPHY/13)

UNDER THE SUPERVISION OF

Dr. VINOD SINGH



DEPARTMENT OF APPLIED PHYSICS
DELHI TECHNOLOGICAL UNIVERSITY
(Formerly Delhi College of Engineering)
SHAHBAD DAULATPUR DELHI-110042

MAY 2021

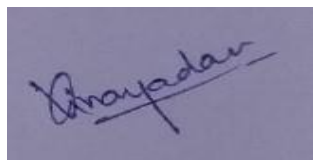
**DEPARTMENT OF APPLIED PHYSICS
DELHI TECHNOLOGICAL UNIVERSITY
(Formerly Delhi College of Engineering)
SHAHBAD DAULATPUR DELHI-110042**

DECLARATION

I, Vinay Kumar Yadav hereby certify that the work which is presented in the Major Project-II/Research work entitled “**Effect of different precursors on morphology of CVD Synthesized MoSe₂**” in fulfilment of the requirement for the award of the degree of **Master of Science in Physics** and submitted to the **Department of Applied Physics, Delhi Technological University, Delhi** is an authentic record of my own, carried out during a period from October 2020 to May 2021, under the supervision of **Dr Vinod Singh**.

The matter presented in this report/thesis has not been submitted by me for the award of any other degree or any other Institute/University. The work has been communicated in SCI/SCI expanded indexed journal with the following details:

| | |
|------------------------------------|---|
| Title of the Paper: | Effect of different precursors on morphology of CVD Synthesized MoSe ₂ |
| Author names: | Vinay Kumar Yadav and Vinod Singh |
| Name of Conference/Journal: | ICDM - 2021 (1st International Conference on Design and Materials - 2021) |
| Status of Paper: | Communicated |
| Date of communication: | 28 th May 2021 |
| Date of Paper acceptance: | |
| Date of publication: | |



**Vinay Kumar Yadav
(2K19/MSCPHY/13)**

DEPARTMENT OF APPLIED PHYSICS

DELHI TECHNOLOGICAL UNIVERSITY

(Formerly Delhi College of Engineering)

Bawana Road, Delhi-110042

CERTIFICATE

I hereby certify that the Project Dissertation-II (MSPH-210) titled “**Study the Effect of different precursors on morphology of CVD Synthesized MoSe₂**” which is submitted by **VINAY KUMAR YADAV**, Roll No **2K19/MSCPHY/13**, Department of Applied Physics, Delhi Technological University, Delhi in partial fulfilment of the requirement for the award of the degree of Master of Science, is a record of the project work carried out by the students under my supervision. To the best of my knowledge this work has not been submitted in part or full for any Degree or Diploma to this University or elsewhere.



30.05.2021

Place: Delhi

Date: 30th May 2021

Project Supervisor

Dr Vinod Singh

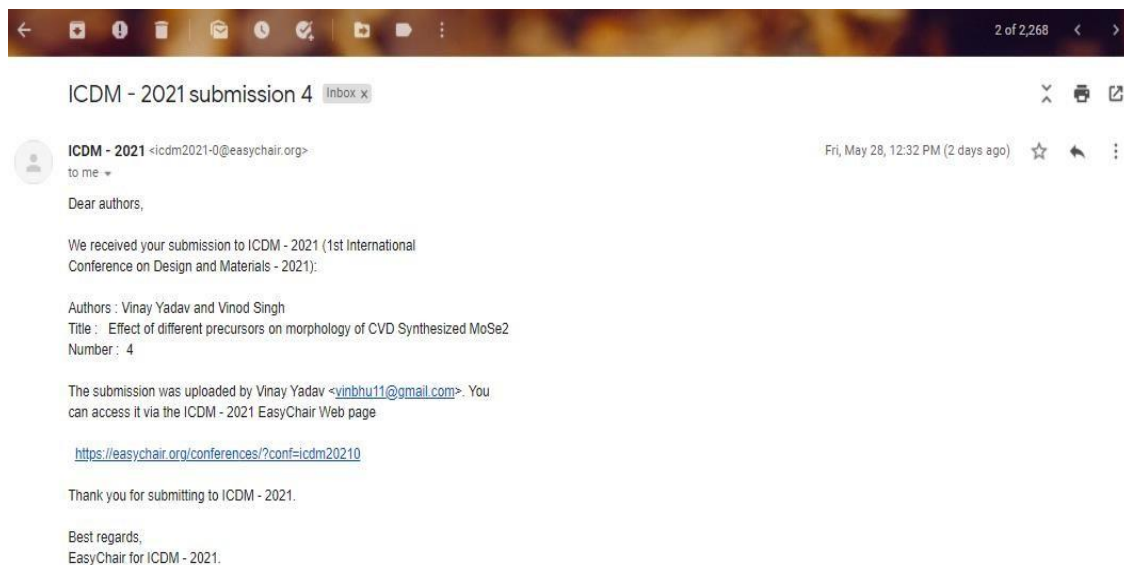
Associate Professor

Department of Applied Physics

Delhi Technological University

Delhi-110042

Communication Record



The screenshot shows an email client interface. At the top, there is a navigation bar with various icons and a page indicator '2 of 2,268'. Below this, the email title is 'ICDM - 2021 submission 4' with an 'Inbox x' tag. The sender is 'ICDM - 2021 <icdm2021-0@easychair.org>' and the recipient is 'to me'. The date and time are 'Fri, May 28, 12:32 PM (2 days ago)'. The email content is as follows:

Dear authors,

We received your submission to ICDM - 2021 (1st International Conference on Design and Materials - 2021):

Authors : Vinay Yadav and Vinod Singh
Title : Effect of different precursors on morphology of CVD Synthesized MoSe2
Number : 4

The submission was uploaded by Vinay Yadav <vinbh11@gmail.com>. You can access it via the ICDM - 2021 EasyChair Web page

<https://easychair.org/conferences/?conf=icdm20210>

Thank you for submitting to ICDM - 2021.

Best regards,
EasyChair for ICDM - 2021.

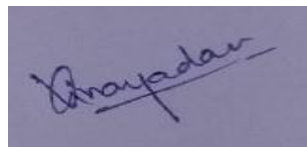
ACKNOWLEDGEMENT

Dissertation-II (MSPH-210) is a golden opportunity for learning and self-development. I consider myself very lucky and honored to have inspiring supervisors who led me in my project.

With due respect and deepest regards, I would like to express my gratitude to **Dr. Vinod Singh** for his encouragement, guidance and motivation throughout this project work. His comments and suggestion have contributed a lot to my work and improved my understanding to the subject.

I am cordially grateful to **Ms. Priya** and Mr. Jasveer Singh for their suggestions and help in lab. I also acknowledge help and support of my lab mates Ms. Shivani Sangwan, Ms. Umang Brewal and Mr. Vivek. I extend my warm regards to all my friends and people who directly or indirectly helped me at NANO FABRICATION TECHNOLOGY LAB, DTU. I also like to thank Mr. Sandeep from Advanced Instrumentation Lab for XRD, DTU.

I would like to thanks my family for guiding me and inspiring me every day to achieve my goals.



Vinay Kumar Yadav

Abstract

Transition metal dichalcogenides (TMD's) emerged as a very appealing candidate for useful implementations in optoelectronics and electronics devices. In two dimensional TMD's materials, MoSe₂ have a direct bandgap (1.1eV) and possess suitable property for optoelectronics devices. Chemical Vapor Deposition (CVD) represents an attractive approach for the growth of MoSe₂ monolayer and nanoflakes. MoSe₂ is synthesized through CVD method and its structural properties are studied. The variation in morphology was also studied by changing growth temperature and precursor ratio. XRD turned into examine the crystal shape and morphology of a freshly produced MoSe₂ sample and found that the synthesized MoSe₂ nanoflakes crystalline size up to 4-5 μ m without any seeding promoter. We changed the growth temperature and flow rate keeping the pressure constant. As result, a slight change in the crystalline size of MoSe₂ is observed. Further when NaCl is used as a seeding promoter and the pressure is reduced, the crystalline size was reduced and observed to be 0.476 μ m.

Contents

| | |
|---|-----|
| Effect of different precursors on morphology of CVD Synthesized MoSe ₂ | 1 |
| DECLARATION..... | i |
| CERTIFICATE..... | ii |
| PLAGIARISM REPORT | iii |
| Communication Record..... | iv |
| ACKNOWLEDGEMENT..... | v |
| Abstract..... | vi |
| List of Figures..... | ix |
| LIST OF TABLES | xi |
| Chapter 1 | 1 |
| Introduction..... | 1 |
| Chapter 2 | 3 |
| About our work..... | 3 |
| 2.1 Our objective | 3 |
| 2.2 Literature Survey..... | 3 |
| 2.2.1 About Molybdenum Selenide (MoSe ₂)..... | 3 |
| 2.2.2 General Synthesis Methodology | 7 |
| 2.2.3 Factor affecting CVD growth..... | 8 |
| 2.2.4 Characterization..... | 10 |
| 2.2.5 EXPERIMENTAL WORK..... | 13 |
| Chapter 3 | 19 |
| Result and Discussion | 19 |
| Chapter 4 | 23 |
| Applications | 23 |
| 4.1 Energy storage..... | 23 |
| 4.2 Photoluminescence | 23 |
| 4.3 Phototransistors | 23 |
| 4.4 Biomedical applications and biosensors | 24 |
| Conclusion | 25 |
| References..... | 26 |
| RESEARCH PAPER | 30 |
| 1 Introduction..... | 30 |
| 2 Experimental Methods | 32 |

| | | |
|----------|------------------------------------|-----------|
| 3 | Result and Discussion | 33 |
| 4 | Conclusion | 36 |

List of Figures

| Fig no. | Name of Figure | Page no. |
|----------------|--|-----------------|
| Fig 2.1 | Formation of hexagonal MoX_2 (X=S, Se or Te) in both states 2H_c and 2H_a | 4 |
| Fig 2.2 | Atomistic model of monolayer MoSe_2 | 4 |
| Fig 2.3 | (a) PL spectra of single-layer, tri-layer and bulk MoSe_2 , (b, c) energy gap diagram of monolayer and bulk MoSe_2 | 5 |
| Fig 2.4 | MoTe_2 phase diagram | 6 |
| Fig 2.5 | Schematic diagram of Chemical Vapor Deposition Method | 8 |
| Fig 2.6 | Diagram of Bragg's diffraction | 10 |
| Fig 2.7 | Diagram of Bragg's diffraction | 11 |
| Fig 2.8 | Thermal split furnace used for sample growth | 15 |
| Fig 2.9 | Schematic diagram of CVD grown MoSe_2 | 15 |
| Fig 2.10 | CVD grown MoSe_2 nanoflakes | 16 |
| Fig 2.11 | CVD grown MoSe_2 thin film on Si/ SiO_2 substrate | 16 |

| | | |
|---------|--|----|
| Fig 3.1 | XRD pattern of CVD grown MoSe ₂ nanoflakes (growth temperature-725°C, Pressure 760 torr) | 20 |
| Fig 3.2 | XRD pattern of CVD grown MoSe ₂ nanoflakes (growth temperature 820°C, Pressure 760 torr) | 21 |
| Fig 3.3 | XRD pattern of CVD grown MoSe ₂ thin film (Growth temperature 750°C, NaCl as seeding promoter, Pressure 30 torr) | 21 |
| Fig 3.4 | XRD pattern of CVD grown MoTe ₂ thin film (growth temperature 700°C, Pressure 760 torr) | 22 |

LIST OF TABLES

| Table no. | Content | Page no. |
|-----------|---|----------|
| 2.1 | Standard values of peak position and Miller indices obtained for MoSe ₂ from XRD data [JCPDS: 87-2419] | 13 |
| 2.2 | Precursors used in Synthesis of MoSe ₂ & MoTe ₂ via Chemical vapor Deposition Method | 17 |
| 3.1 | Calculated Interplanar spacing, Crystalline size and Lattice parameter of MoSe ₂ | 19 |

Chapter 1

Introduction

In this development era, graphene and two-dimensional (2D) substances have emerged because the maximum promising contender toward future electronics because of unique structure, physical property, high carrier mobility, and low resistivity [5]. The non-appearance of the bandgap in graphene has blocked its use in a logic circuit. This non-appearance of bandgap makes, difficult to control the on/off current in graphene transistors so turning off the graphene-based transistor is a difficult task. This disagreeable property of graphene provoked research on its subordinates and other 2D layered nanomaterials [1]. TMD substances have been perceived to engross up to 5%-10% of incident daylight within a depth of < 1 nm, which is approximately an array of significance better in comparison of GaAs and Si. Transition Metal Dichalcogenides (TMD's) possessing 2D Van Der Waals heterostructure and outstanding properties ranging from insulator to metal. A thin layer of TMD's with ratio MX_2 (M= transition metal of group IV-X, X=S, Se or Te) having properties such as strong spin-orbit coupling, ferromagnetism, quantum spin hall effect, tunable band structure, conventional superconductivity & quantum confinement structure to use for various application in optoelectronics, electronics, energy storage, and photonics [3,5,6,18]. 2D substances show excellent light interaction over a bandwidth from to infrared to ultraviolet wavelength and permit photodetection on this bandwidth.

TMD's, usually single layer shows two distinct crystal structure due to electronic structure. One is trigonal prismatic symmetry(1H/2H) and the octahedral symmetry. In transition metal, alteration of electron agreement in the d orbital, octahedral geometry expands into a distorted octahedral symmetry(1T') [11]. The range of layers and defects have a considerable impact on the properties and applications of TMDs. Highly imperfect TMDs, for example, are extraordinary beneficial in catalysis applications. However, no complete switch over crystal size, layer range, or disorder has yet been confirmed in an experiment [12].

In the same range of applications, MoSe₂ has lately proven more promise. Metal selenides, in general, have recently been investigated as viable dilemma to ordinary metal sulphides for energy storage [3]. The indirect bandgap is 1.1 eV, in bulk MoSe₂, and in single -layer MoSe₂, the direct bandgap is 1.5 eV [2]. MoSe₂ has a bandgap close to that of Si (1.12 eV), making it suitable for use in optoelectronics and photocatalysts. The main benefit of MoSe₂ aloft MoS₂ is that it has a surpassing electrical conductivity due to Se's inherent metallic existence (10^{-3} s m⁻¹ vs. 0.5×10^{-27} s m⁻¹ for sulphur). Sulphur defects in the MoS₂ monolayer are known to have a critical impact on electronic transport and optical properties [3]. As a result, a careful comparison of the properties of monolayer MoS₂ and MoSe₂ would be useful. MoSe₂ can take the form of nanoflakes, nanofilms, & nanoflowers.

MoSe₂, like other TMDCs like MoS₂, may have a number of different of phase structures, including 2H trigonal prismatic (semiconducting in nature) and 1T octahedral (metallic in nature). The metallic 1T MoSe₂ is thermodynamically unsteady, switching into 2H MoSe₂ (semiconducting) all through time. This implies that, while MoSe₂ (metallic) is more appropriate for a variety of applications, but it is not beneficial to utilize [3]. MoSe₂ (semiconducting) has recently acquired a number of interests for its potential applications in electrochemical, optoelectronic, chemical sensors, photocatalytic and biosensor technologies [3,4]. Since the vulnerable van der Waals (vdw) dynamics can be triumph over to separate different surface of MoSe₂, similar to graphene, so this opens up a wide range of optoelectronic utilization, such as LED's, optical sensors, light harvesting and so on [3].

Chapter 2

About our work

2.1 Our objective

In this work, we used Thermal Chemical Vapor Deposition (CVD) method to synthesize the MoSe₂ thin film samples and nanoflakes. The nanoflakes sample quantity was adequate for satisfactory analysis, so all of the samples have been characterized through X-Ray Diffraction techniques. Further the morphology evaluation of the CVD grown MoSe₂ nanoflakes is discussed in this article. The ultimate intention is to evaluate how close our findings fit to the usual data of MoSe₂ lattice parameters, and therefore discuss on its morphology evolution with the alternate of precursor under ambient pressures.

2.2 Literature Survey

2.2.1 About Molybdenum Selenide (MoSe₂)

The discrete layers of MoSe₂ are assembled collectively through vdw's interactions in a two-dimensional lattice formation. Since this structure is close to that of graphite, this elegance of substances can reasonably simulate graphene or graphite applications. MoSe₂ can have a variety of phase structures. The electronic states of d-orbital of Mo atoms pair the MoSe₂ layers with diatomic arrangement. Polymorphs like 2H_a and 2H_c can be formed as a result of layer stacking [3]. The phase transition between these structures is also a possibility. The vdw's dynamics of the surface and the coulomb interaction of Mo and Se withinside the nearest-neighbor surface of Mo in both states are active contestants in computational calculations of MoSe₂, ensuing in resistance to the traditional state transition allying 2H_c and 2H_a.

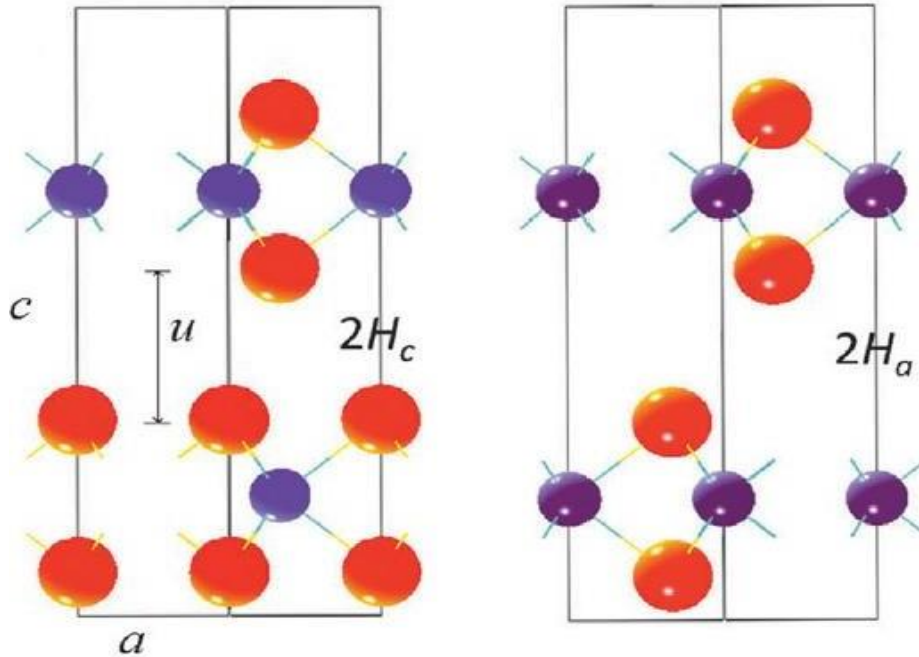


Fig 2.1^[29]: Formation of hexagonal MoX₂ (X=S, Se or Te) in both states 2H_c and 2H_a

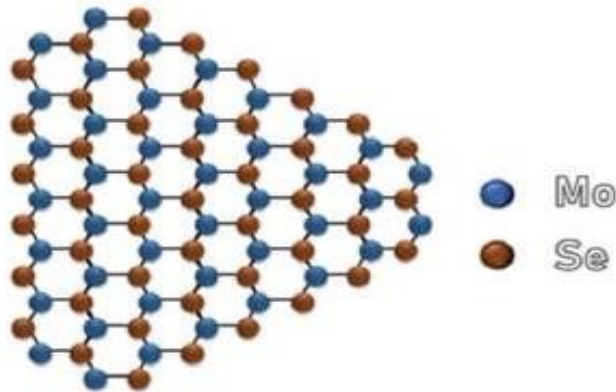


Fig 2.2: Atomistic model of monolayer MoSe₂

MoSe₂ is a type of stacked substance expressed by the MX₂ general TMDs formula, where M and X represent Mo and Se, respectively. The atoms of Mo and Se form a covalent bond and form the Se-Mo-Se basic sheet. MoSe₂ is organized in a sandwich 2D shape with interlayer spacing of 6.5Å by stacking Se-Mo-Se surfaces on top of one to another and connecting them through vdw's dynamics [4]. Bilayer MoSe₂ grains have an AA layer shape (the relative turn perspective of two in an upward direction stacked triangles $\theta = 0^\circ$), but there is also some AB stacking bilayer (the overall pivot point $\theta = 60^\circ$), hexagonal bilayer, and tri-layer grains, which

can likewise infer that the AA stacking order is greater favorable at lower growth temperatures [17].

Since it exhibits many of the same optical and electronic characteristics as monolayer MoS₂, for example a direct band gap, high photoluminescence (PL), and a high exciton restriction energy, monolayer MoSe₂ has tended to grab interest. MoSe₂ has a narrow bandgap. In bulk MoSe₂, the indirect bandgap is 1.1 eV, and the direct bandgap is 1.5 eV in single-layer MoSe₂, with an energy gap close to Silicon's (Si) energy gap (1.12 eV) [2].

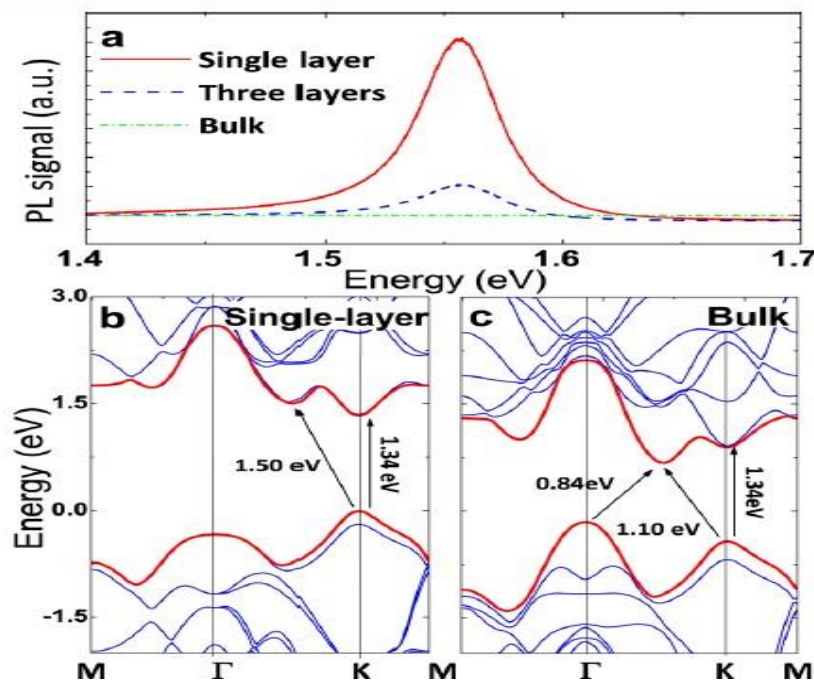


Fig 2.3²: (a) PL spectra of single-layer, tri-layer and bulk MoSe₂, (b, c) energy gap diagram of monolayer and bulk MoSe₂

MoSe₂ is an indirect bandgap semiconductor with a bandgap value of 1.1 eV in the bulk limit, so the bandgap PL is assumed to be small. In a few layer MoSe₂ flakes, the PL intensity gradually increases ~1.5-1.6 eV, and the PL crest intensity reaches its most extreme incentive for a single-layer MoSe₂, as shown in Fig 2.3.(a). Bulk MoSe₂ has indirect bandgaps of 8.4×10^{-1} eV Γ to Γ -K, 0.11×10^{-1} eV K to Γ -K, and a direct bandgap of 1.34 eV K to K. (Fig 2.3.c). Single-layer MoSe₂, on the other hand, increases from to K to Γ -K and K to Γ -K, while the K-K energy gap residue practically unrelated, and MoSe₂ becomes a direct energy gap semiconductor with a 1.34 eV energy gap value at the K symmetry level (Fig 2.3.b) [2].

CVD grown MoSe₂ based fabricated FETs have average carrier mobility ranging from 8 to 38 cm²/V. s, and phototransistor high photoresponsivity ~100 A/W, external quantum efficiency of 23.5% and much faster response time (<25ms) [13,16]. The MoSe₂ has a modest n-type ambipolar tendency, where the MoS₂ has electrical properties with strongly n-doped.

In comparison of MoSe₂, **MoTe₂** synthesizes into different phases, α-phase (or 2H phase, trigonal prismatic structure), β-phase (or 1T'-phase, monoclinic structure, distorted octahedral) & γ-phase (or T_d-phase, orthorhombic structure) [21].

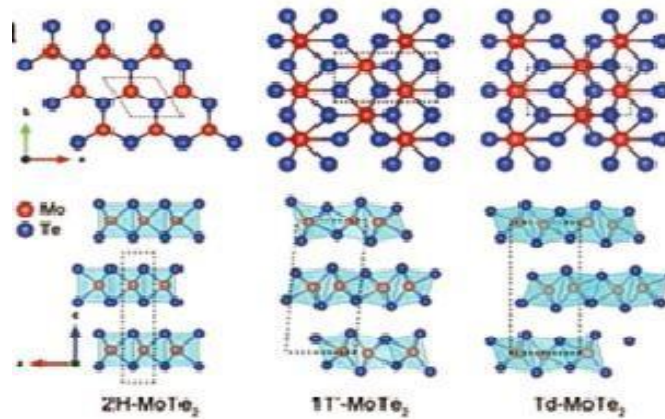


Fig 2.4: MoTe₂ phase diagram

A 2H phase of MoTe₂ has a direct bandgap close to silicon (Si) that is ~ 1.1eV and carrier mobility > 2500 cm².V⁻¹.s⁻¹ at room temperature (R_T) [27], so it is a promising replacement for Si applicants, in the future. 2H- MoTe₂ having properties such as strong spin-orbit coupling & thermoelectric. Physicists are interested in 1T' phase MoTe₂ due to its narrative feature such as large magnetoresistance, pressure-driven superconductivity. In bulk form of 1T' - MoTe₂ has high mobility ~ 4000 cm².V⁻¹.s⁻¹, and large magnetoresistance ~ 16000% in 14 tesla of the magnetic field at 1.8 K [26]. Recently conversion of 2H - MoTe₂ to 1T' - MoTe₂ was reported [25]. 2H and 1T' phases of MoTe₂ easily coexist under normal conditions, and the ground state energy allying these two states is quite small (<0.1eV) [24]. The monoclinic 1T' - MoTe₂ is a semimetal that goes through underlying progress into an orthorhombic γ-phase, introduced as the T_d phase, at around 240 K [23]. Ongoing hypothetical and an exploratory investigation dependent on angled resolved photoemission spectroscopy have uncovered that MoTe₂ has type II Weyl semimetal fermions [21,22].

Molybdenum (Mo) based dichalcogenides are used in energy storage (Lithium ion batteries) due to their sandwich structure. MoSe₂ and MoS₂ have small interlayer distance (0.65nm & 0.32nm) between their layer and both suffer huge lattice deformation during infusion and extraction of Na⁺ ion, which promote shape uncertainty. Molybdenum di-telluride (MoTe₂) has an interlayer spacing about 0.70 nm, with unique structure and tunable properties and has potential to use for electrode in sodium ion batteries (SIBs) [20] and Lithium ion batteries (LIBs) [19]. A full cell (MoTe₂ as anode, in SIBs) show high capacity with high rate potential (207 mAh g⁻¹) and exceptional cycling stability (88% reversible capacity retentiveness after 150 cycle) has been fabricated [20]. 2H-MoTe₂ electrode (anode, in LIBs) reveal high potential (of 432 mAh g⁻¹) and capacity retentiveness of 80% above 100 cycles [19].

2.2.2 General Synthesis Methodology

To the synthesis of, 2D TMDs materials, various methods are available, such as chemical vapor deposition, Hydrothermal method, mechanical/chemical exfoliation and chemical vapor transport methods [3,4,10,11,12,14,15,17].

The **Chemical vapor deposition (CVD)** approach is a vapor-phase grow approach and can be divided into two kinds. At first, the source substance is coated atop the substrate earlier before the growth, that is called the two-step technique. In second, source material can be used separately instead of coating on the substrate, which is called the one-step technique. In synthesis by a CVD method, few factors are affecting, namely, precursors (source materials), heating temperature, growth time, flow rate, and composition of the carrier gas. The CVD method consists of three steps of 1-Evaporation, 2-Transport, and 3-Growth [28]. In step one, craved product elements are available in solid powder form as precursors. When we heat, after sufficient temperature precursors, start to evaporate for the chemical reaction. In step two, the transportation of evaporated precursors needs carrier gases (inert gases, such as Ar), for chemical vapours to reach the substrate surface. Additional gas, such as H₂, is induced to sustain the deposition process. In step three, when the chemical vapours reach the substrate surface, a reaction takes place and the growth of the desired material proceeds at a certain temperature.

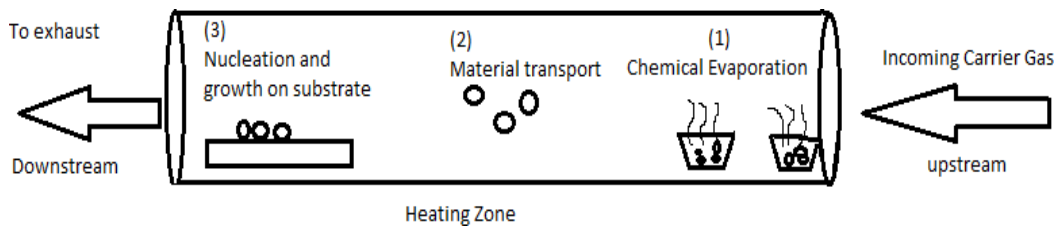


Fig 2.5: Schematic diagram of Chemical Vapor Deposition Method

2.2.3 Factor affecting CVD growth

- Chemical precursors-** The selection of precursors and their attentiveness represent an important role in growth. The precursor used for synthesis is the metal oxide (MoO_3 , WO_3), chalcogen powder (S, Se, and Te), and solution-based/powder source as MoCl_5 . In deciding, the excellence of grown MoSe_2 , Mo precursor plays an important role. Choosing MoO_3 as a precursor because it possesses some unique qualities such as MoO_3 starts to sublimed at around $397\text{-}497^\circ\text{C}$ (melting point: 795°C). MoO_3 can absorb moisture and the moisture could be accrued and assist to make a more uniform film.
- Heating temperature** - Temperature holds vaporization temperature & growth temperature, in CVD approach. Temperature affects the vapor pressure of the precursor, and increases the rate of reaction with increasing temperature. By temperature, not only the crystal of material affected but also its interaction with the substrate also affected.
- Growth time-** Growth time is most important for the chemical reaction. For large area film growth, we have to maintain growth time either 15-20 minutes.
- Flow rate and composition-** The flow rate and the composition of carrier gas constitute a crucial role in the growth of 2D TMDs not at most transport precursor vapor to substrate surface but also prevent the

oxidization during growth. H₂ gas presence, help in the growth of 2D TMDs [30]. Chemical reaction density can be additionally constrained by the gas flow rate because the rate of transport of chalcogen is constrained by the gas flow rate.

- **Nucleation Density-** The nucleation density is the primary determinant of crystal size. Since the flowrate specifies the amount of Se vapour introduced to the reaction, tuning the flowrate of carrier gas with a set temperature of Se will regulate the nucleation density. One of the most common techniques for developing the nucleation density for graphene growth is to control the quantity of reactant used. The nucleation density of MoSe₂ layers can be decreased from 105 to 25 core cm⁻² using a chemical vapour deposition method, resulting in millimetre-parameter MoSe₂ mono crystals in addition continuous macro crystalline films with millimetre-sized grains [31].
- **Effect of Hydrogen gas-** H₂ is often used in CVD systems to increase the substance reactivity of chalcogenide antecedents and the excellency of TMD materials including MoSe₂ and WS₂. H₂ facilitates sulphurisation (selenization/tellurization) by speeding up the reduction of metal oxide. The primary product in an argon environment is few-layer MoSe₂ grains and MoO_x nanograins, however, when H₂ was introduced, monolayer MoSe₂ have become the dominant product all through CVD development [30]. We added hydrogen gases with various stream rates into the CVD system to prevent the development of MoO_x as a side product and to work with the growth of high-quality, monolayer MoSe₂ grains.

The **Hydrothermal Synthesis** process involves a series of physicochemical reactions between precursor materials namely molybdate and sulphur in a stainless-steel autoclave. These reactions take place in a high pressure, high temperature environment for several hours. The obtained MoSe₂ nanoflakes/powder is subjected to annealing to enhance its crystallinity and purity. This method allows for some control over the size of individual particles by changing suitable reaction parameters [15].

The **Liquid phase exfoliation (LPE)** is a quick and easy way to get materials with a lot of surface area. Mass MoSe₂ diffused in the fluid will be divided into many layers with broad

surface region using agitations such as shear, ultrasonication, and heat in the liquid phase method, resulting in MoSe₂ nanosheets [4].

CVD is the most effective in the numerous growth techniques for 2D layers for realising high-quality and wafer-scale 2D substances. Mechanical exfoliation, for example, has the disadvantages of low yield, poor reproducibility, and limited scale [12].

2.2.4 Characterization:

X-ray Diffraction (XRD)- The reticular planes that shape the atoms of the crystal cause diffraction, which is one of the effects of X-ray contact with crystalline matter. Depending on the wavelength, orientation of crystal, with composition, the diffracting beam moving along it to emit rays at various values of theta.

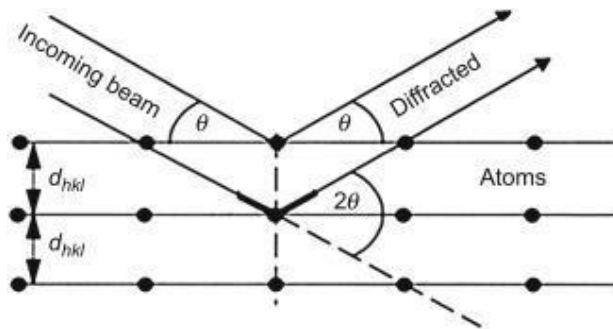


Fig 2.6: Diagram of Bragg's diffraction

A certain value of λ of the incident ray can produce a synchronizing interference pattern when partially reflected among different surfaces that create a path difference equal to an integral value of the wavelengths in the macroscopic version of the diffraction pattern. The Bragg law describes this scenario as follows:

$$2d \sin\theta = n\lambda \quad \dots\dots (2.1)$$

where n is diffraction order, λ is value of x-ray' wavelength, d is the gap between the successive layers of atom, and θ is the glancing angle. This relationship shows these effects are visible when interaction among the physical measurements and radiation occurs that are close to the

wavelength of the radiation. Diffraction methods have wavelengths that are similar to the wavelength of X-ray, since the distances between lattice constituents are generally atomic 10^{-10}m (1Å).

Dimensions of crystallites

Peak broadening and nano crystallite size are associated, because the diffraction peak width will reveal details about the material's microstructure. Furthermore, lattice defects and strain can influence peak broadening. Depending on the form of curve fitting, this measured by integral breadth and FWHM. For our analysis, we used the FWHM values provided by Origin software and applied the equation (2.2) (Scherrer) to obtain the size of the crystallite:

$$D_{hkl} = K\lambda/\beta_{2\theta} \cos\theta \quad \dots\dots (2.2)$$

Where,

K: a constant that is called Scherrer constant (shape factor)

λ : wavelength, β : width of the diffraction crest, given in radians

θ : Bragg angle

Crystallite size broadening is proportional to $1/\cos\theta$.

Lattice constants

The usually exploited phenomenon in X-Ray diffraction technique is the Bragg's diffraction, whereby constructive interference of waves scattered from lattice planes having high electron densities (Bragg's planes) results in sharp, intense Bragg's peaks. For constructive interference to take place from lattice planes separated by distance d , the following condition, well known as the Bragg's Law must, be satisfied:

$$2d\sin\theta = n\lambda$$

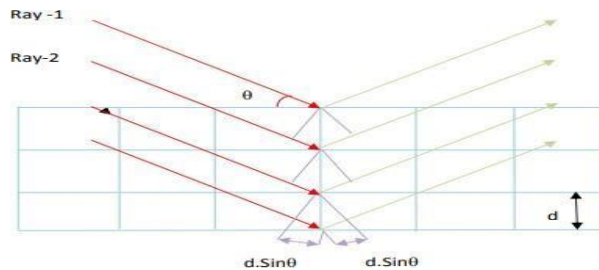


Fig 2.7: Diagram of Bragg's diffraction

In usual diffraction experiments, a set wavelength is used (given property- 1.5Å in our experiment); the d-spacings are the unknown characteristics of the sample to be analyzed, at the same time the diffraction angles are the ensuing observed characteristics. Measuring the intensity of scattered waves as a function of scattering angle results in a diffraction shape in which the determined angular positions of the diffraction peaks (for a given wavelength) provide statistics about the unit cell metrics of a crystalline substance.

For hexagonal structures, the interplanar spacing d, (a, c) the constants of the lattice and (h, k, l) the indices of the lattice as per by miller are related by the equation:

$$\frac{1}{d^2_{hkl}} = \left(\frac{4}{3}\right)\left(\frac{h^2+hk+k^2}{a^2}\right) + \frac{l^2}{c^2} = \frac{4\sin^2\theta}{\lambda^2} \dots\dots\dots (2.3)$$

Rearranging with n=1 estimation gives:

$$\sin^2\theta = \frac{\lambda^2}{4} \left[\frac{4}{3} \left(\frac{h^2+hk+k^2}{a^2} \right) \right] \dots\dots\dots (2.4)$$

For cell shaped like hexagons, a can be calculated looking at type of plane similar to (h k 0).

Substituting l=0 in equation, in result:

$$a = \frac{\lambda}{(\sqrt{3})\sin\theta} \sqrt{h^2 + hk + k^2} \dots\dots\dots (2.5)$$

And c can be calculated when h=k=0 and using the formulae give below:

$$c = \lambda / 2\sin\theta \dots\dots\dots (2.6)$$

Table 2.1: Standard values of peak position and Miller indices obtained for MoSe₂ from XRD data [JCPDS: 87-2419]

| S. No. | Peak position (2θ, degrees) | Miller Indices | | |
|--------|-----------------------------|----------------|---|---|
| | | h | k | l |
| 1 | 13.686 | 0 | 0 | 2 |
| 2 | 27.572 | 0 | 0 | 4 |
| 3 | 41.887 | 0 | 0 | 6 |
| 4 | 57.824 | 1 | 1 | 4 |
| 5 | 69.472 | 2 | 0 | 3 |

2.2.5 EXPERIMENTAL WORK

Reagents and materials

In a quartz tube, in split furnace, Molybdenum trioxide (MoO₃) powder (99.99% purity, Sigma Aldrich), selenium (Se) powder and pure sodium chloride (NaCl) crystal were used as precursors. For transporting vaporised materials to a silica (SiO₂) substrate, argon and hydrogen were used as carrier gases. All of the boats, beakers, and crucibles employed in the sample preparation went through a normal rinsing process that included dilute acid/acetone cleaning followed by ultrasonic cleaning, as detailed below.

Cleaning Procedure

The quartz tube was very well rinsed with sulphuric acid/acetone prior to placement in the reaction chamber, and the wafer/substrate container was cleaned with organic solvents including acetone and ultrasonically cleaned. To extract all residual dirt from the material, an ultrasonic cleaning in Acetone was performed for around 15-20 minutes.

Growth of MoSe₂

The whole reaction took place in a split furnace in a 1.3-inch depth of quartz tube. MoSe₂ was obtained by selenization of MoO₃ powder. 10-20 mg MoO₃ powder (99.99% purity, Sigma Aldrich) containing in a boat (made of ceramic) located at the centre of the furnace, and 0.4-0.5g Se powder (99.99% purity, Sigma Aldrich) in another ceramic boat was located upstream of furnace 12-15cm away from the centre. a cleaned 2cm×2cm dimension, 300nm SiO₂/Si substrate placed in MoO₃ containing boat 3-5cm away from the MoO₃ powder towards downstream. A mixture of H₂ and Ar gas flow during the whole reaction, used as carrier gas (5 s.c.c.m. H₂ + 60 s.c.c.m. Ar). The furnace was heated up to 720-880°C with a ramping rate of 14°C/min and kept steady at this temperature for 15 min. After the whole reaction was completed led the furnace cooled right all the way down to room temperature naturally.

Growth of MoTe₂

The whole reaction took place in a split furnace in a 1.3-inch depth of quartz tube. MoTe₂ was obtained by tellurization of MoO₃ powder. 50-60 mg MoO₃ powder (99.99% purity, Sigma Aldrich) containing in a boat (made of ceramic) located at the centre of the furnace, and 5g e powder (99.99% purity, Sigma Aldrich) in another ceramic boat was located upstream of furnace 7-10cm away from the centre. a cleaned 2cm×2cm dimension, 300nm SiO₂/Si substrate placed in MoO₃ containing boat 3-5cm away from the MoO₃ powder towards downstream. A mixture of H₂ and Ar gas flow during the whole reaction, used as carrier gas (5-15 s.c.c.m. H₂ + 80-85 s.c.c.m. Ar). The furnace was heated till 700°C with a ramping rate of 18°C/min and kept steady at this temperature for 20 min. When the whole reaction was completed led the furnace cooled right all the way down to room temperature naturally.



Fig 2.8: Thermal split furnace used for sample growth

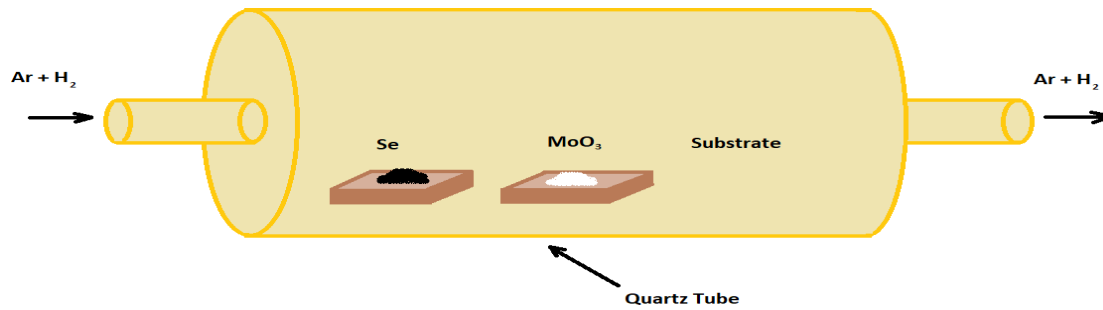


Fig 2.9: Schematic diagram of CVD grown MoSe₂



Fig 2.10: CVD grown MoSe₂ nanoflakes



Fig 2.11: CVD grown MoSe₂ thin film on Si/SiO₂ substrate

Table 2.2: Precursors used in Synthesis of MoSe₂ and MoTe₂ via Chemical vapor
Deposition Method

| Precursor | Flow rate | Growth Temp. | Growth Time | Resultant |
|-------------------------------------|--|--------------|-------------|---|
| MoO ₃ & Se Powder | 63 sccm Ar + 5 sccm H ₂ & Pressure 760 torr | 725°C | 15 min | MoSe ₂ powder form in crucible |
| MoO ₃ & Se Powder | 70 sccm Ar + 10 sccm H ₂ & Pressure 760 torr | 850°C | 20 min | Thin film & MoSe ₂ nanoflakes |
| MoO ₃ , NaCl & Se Powder | 50 sccm Ar + 5 sccm H ₂ & Pressure 30 torr | 750°C | 15 min | Thin film & MoSe ₂ nanoflakes |
| MoO ₃ , Te powder | 80 sccm Ar + 5 sccm H ₂ & Pressure 760 torr | 700°C | 20 min | Thin film or powder we were expecting |

| | | | | |
|-------------------------------------|--|-------|--------|---------------------------------------|
| MoO ₃ , NaCl & Te powder | 85 sccm Ar + 15 sccm H ₂ & Pressure 760 torr | 700°C | 20 min | Thin film or powder we were expecting |
|-------------------------------------|--|-------|--------|---------------------------------------|

Chapter 3

Result and Discussion

The crystal shape and phase evolution of the resulting MoSe₂ sample were confirmed using an X-ray diffractometer. The XRD characteristic of the resulting MoSe₂ nanoflakes are shown in Fig 3.1-3.3. Diffraction peaks observed in a scale of 5–80 degrees on the X-ray diffractogram for the MoSe₂ & MoTe₂ sample. The diffraction peaks detected in the MoSe₂ sample's XRD spectrum reveal a hexagonal crystal shape with growth direction ahead one axis (101). The reported d-spacing values and lattice variables align well with previous research [JCPDS: 87-2419], which mentioned in below table.

Table 3.1 Calculated Interplanar spacing, Crystalline size and Lattice parameter of MoSe₂

| Sample | Position (2θ) | Interplanar spacing 'd' (Å) | Crystalline size 'D' (Å) | Lattice parameter |
|--------|--|--|--|--|
| 1) | 13.68 27.46 32.16 41.32 57.83 72.47 | 6.47 3.24 2.78 2.18 1.59 1.30 | 488.56 384.50 514.42 29480.19 513.65 627.01 Avg 5334.72 Å Or 5.33 μm | a=b= 0.277nm & c= 1.29 nm |
| 2) | 13.62 32.15 56.33 69.48 | 6.4 2.78 1.63 1.35 | 4684.27 509.62 11582.65 413.16 Avg- 4297.42Å or 4.3μm | a=b= 0.277nm & c= 1.29nm |

| | | | | |
|----|------------------------|----------------------|---------------------------------------|---|
| 3) | 27.53 32.14 59.6 | 3.24 2.78 1.55 | 419.47 434.07 574.59 | a=b= 0.277nm & c= 1.29nm |
| | | | Avg- 476.04Å or 0.476µm | |

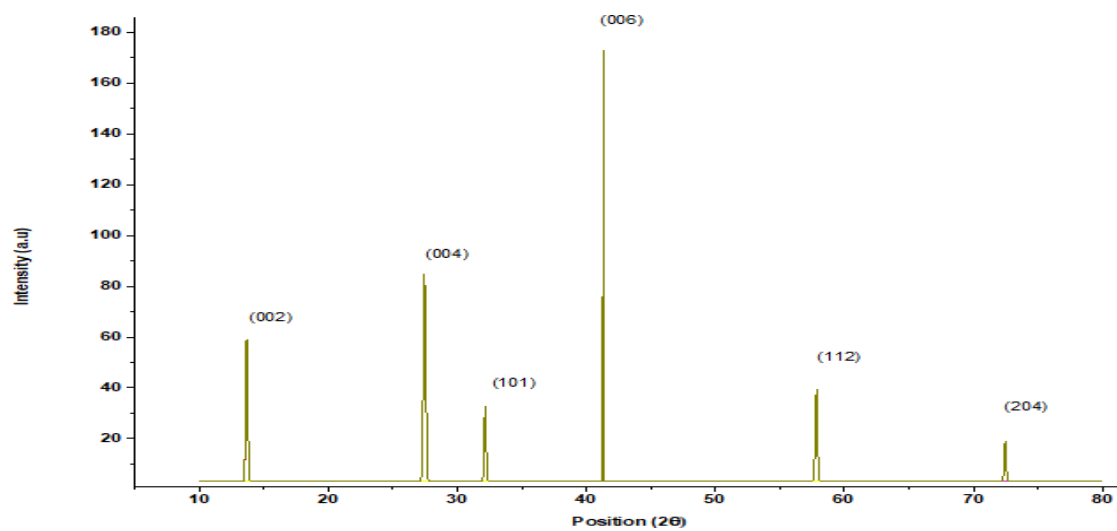


Fig 3.1: XRD pattern of CVD grown MoSe₂ nanoflakes (growth temperature-725°C, Pressure 760 torr)

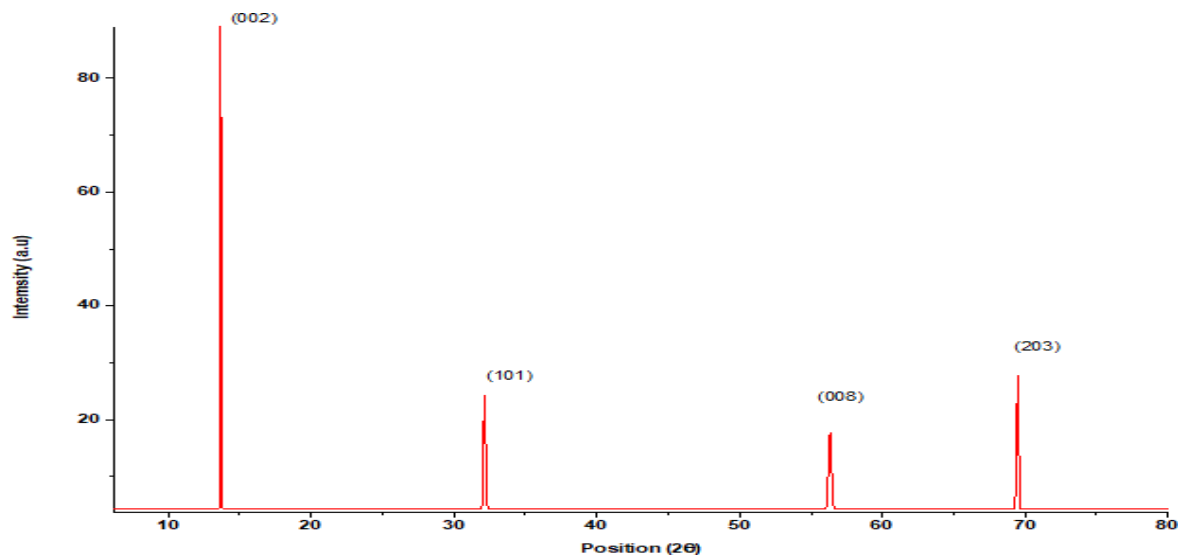


Fig 3.2: XRD pattern of CVD grown MoSe₂ nanoflakes (growth temperature 820°C, Pressure 760 torr)

In samples 1 and 2 we change the gas flow rate and growth temperature (kept pressure constant 760 torr), from the XRD data we can say that in both samples MoSe₂ nanoflakes formed uniformly with the crystalline size of 5.335 μ m and 4.297 μ m respectively, and doesn't show much crystalline size difference.

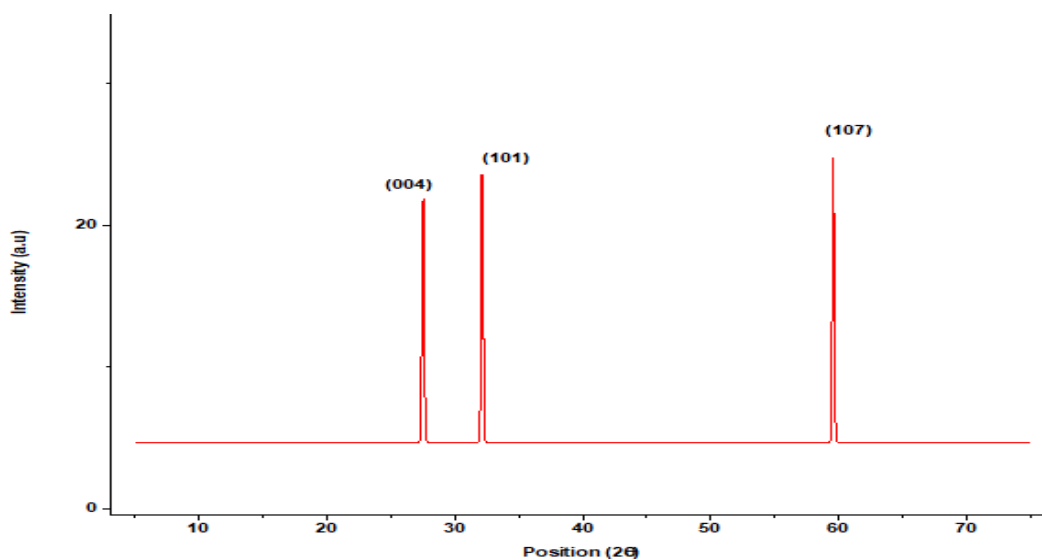


Fig 3.3: XRD pattern of CVD grown MoSe₂ thin film (Growth temperature 750°C, NaCl as seeding promoter, Pressure 30 torr)

In the same way, when we synthesized NaCl assisted MoSe₂, we reduced the pressure to 30 torr, we found the crystalline size reduced and become 0.476 μ m. here, we were using NaCl as a growth promoter, as it is an oxidizing agent, so reduced the temperature of reaction [12], but it has been observed that there is a major difference of this much in crystalline size.

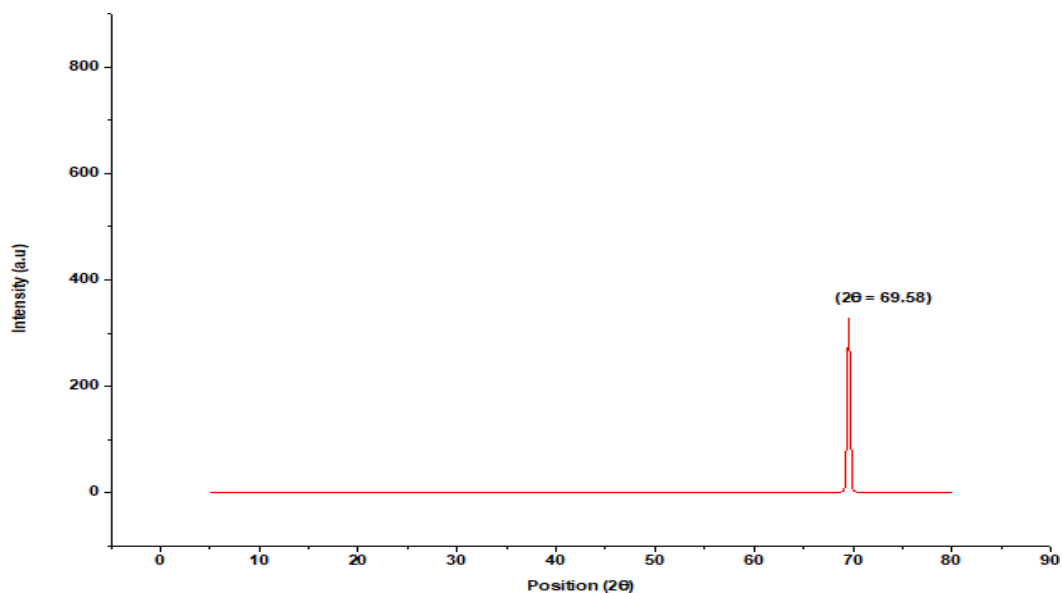


Fig 3.4: XRD pattern of CVD grown MoTe₂ thin film (growth temperature 700°C, Pressure 760 torr)

We tried to synthesize MoTe₂ via CVD approach with seeding promoter and without seeding promoter and expecting thin film deposition of MoTe₂ on substrate but XRD data reveals only a dominating peak of substrate. The Sublimation temperature of MoO₃ & Te is higher in comparison of Se and S and in our furnace system we didn't achieve in this experiment. Also, pressure effect which is required high to perform this experiment we could not achieve so synthesis of MoTe₂ is not successful. It is possible if we would have if metal oxide deposited substrate so we have to perform only tellurization process.

Chapter 4

Applications

4.1 Energy storage-

- **Lithium-ion batteries:** As compared to MoS₂, MoSe₂ has a greater layer spacing, so it should do better in intercalation systems. The MoSe₂ reveals the identical electrochemical steadiness as the MoS₂. The primary distinction allying MoS₂ and MoSe₂ is that in the case of MoSe₂, a well-described redox mechanism appears, as reveal by a level in galvanostatic profiles and a very much formed peak couple in cyclic voltammograms. The cyclability of the carbon nanocomposites was substantially improved after the initial cycles, while pure MoSe₂ ought to achieve an excessive unique potential with just 20% less [3].
- **Sodium-ion batteries:** Because of its broad interlayer spacing (at least in contrast to MoS₂), MoSe₂ is well acceptable to hosting large alkali metallic cations which including Na. The structural change caused by Na intercalation results in the formation of metallic Mo and Na₂Se (as in lithium-ion storage device), even as the fullerene-like crate constructed by CNT's holds the electro-active substances in place. In resultant, the electrode's strength turned into maintained after 50 cycles [3].

4.2 Photoluminescence- MoSe₂ has a direct bandgap that is similar to the ideal value needed for photo-electrochemical and solar cells. As the width of this 2D shape is decreased to a mono or a few layers of MoSe₂, substance's indirect and direct bandgaps become nearly degenerate [3,15].

4.3 Phototransistors- The phototransistor primarily based totally on MoSe₂ has a far quicker reaction time (25 ms) than the CVD MoS₂ phototransistor (which takes 30 s), monolayer in atmospheric conditions at room temperature. Under the illumination of light, a MoSe₂ thin film transistor with a moderately high field-impact carrier mobility (8-38 cm²/V. s) well known shows a high photoresponsivity (~100 A/W) and a short photo response time, demonstrating the functional feasibility of multilayer MoSe₂ thin film transistors for photodetector applications [8,9,13,15,16].

4.4 Biomedical applications and biosensors- Since MoSe₂ has a higher electrical conductivity and electro catalytic activity than MoS₂, it can perform better in electrochemical sensors. Although no fundamental research into the precise electrochemical reaction of MoSe₂ in bio-detecting frameworks has been published, MoSe₂ has currently been used to fabricate a variety of electrochemical(bio) sensors [4].

Conclusion

We used CVD techniques to synthesis of MoSe₂ nanoflakes. XRD turned into used to analyse the crystal structure and shape of a freshly produced MoSe₂ sample and found that the synthesized MoSe₂ nanoflakes crystalline size up to 4-5 μ m without any seeding promoter. we change the growth temperature and flow rate but kept the pressure constant. In resultant, there is a slight difference in the crystalline size of MoSe₂. But when we use the seeding promoter (NaCl) kept the same condition but reduced the pressure, the crystalline size was reduced and obtained 0.476 μ m. We conclude that CVD grown MoSe₂ changes with the change of precursor ratio, gas flow rate, growth rate and pressure.

References

1. Kumar, A., Ahluwalia, P.K. Electronic structure of transition metal dichalcogenides monolayers $1H-MX_2$ ($M = Mo, W$; $X = S, Se, Te$) from ab-initio theory: new direct band gap semiconductors. *Eur. Phys. J. B* **85**, 186 (2012). <https://doi.org/10.1140/epjb/e2012-30070-x>.
2. Sefaattin Tongay, Jian Zhou, Can Ataca, Kelvin Lo, Tyler S. Matthews, Jingbo Li, Jeffrey C. Grossman, and Junqiao Wu, Thermally Driven Crossover from Indirect toward Direct Bandgap in 2D Semiconductors: $MoSe_2$ versus MoS_2 , *Nano Letters* **2012** 12 (11), 5576-5580, DOI: 10.1021/nl302584w.
3. Ali Eftekhari, "Molybdenum diselenide ($MoSe_2$) for energy storage, catalysis, and optoelectronics", *Applied Materials Today*, Volume 8, 2017, Pages 1-17, ISSN 2352-9407, <https://doi.org/10.1016/j.apmt.2017.01.006>.
4. Fan Jiang, Wen-Sheng Zhao, Jun Zhang, Mini-review: Recent progress in the development of $MoSe_2$ based chemical sensors and biosensors, *Microelectronic Engineering*, Volume 225, 2020, 111279, ISSN 0167-9317, <https://doi.org/10.1016/j.mee.2020.111279>.
5. Yang L, Xie C, Jin J, Ali RN, Feng C, Liu P, Xiang B. Properties, Preparation and Applications of Low Dimensional Transition Metal Dichalcogenides. *Nanomaterials* (Basel). 2018 Jun 26;8(7):463. doi: 10.3390/nano8070463. PMID: 29949877; PMCID: PMC6071048.
6. Manas Ranjan Panda, Anish Raj K, Arnab Ghosh, Ajit Kumar, Divyamahalakshmi Muthuraj, Supriya Sau, Wenzhi Yu, Yupeng Zhang, A.K. Sinha, Matthew Weyland, Qiaoliang Bao, Sagar Mitra, Blocks of molybdenum ditelluride: A high rate anode for sodium-ion battery and full cell prototype study, *Nano Energy*, Volume 64, 2019, 103951, ISSN 2211-2855, <https://doi.org/10.1016/j.nanoen.2019.103951>.
7. [Titao Li](#), [Zhaojun Zhang](#), [Wei Zheng](#), [Yangyang Lv](#), and [Feng Huang](#), "A possible high-mobility signal in bulk $MoTe_2$: Temperature independent weak phonon decay", *AIP Advances* 6, 115207 (2016) <https://doi.org/10.1063/1.4967351>.
8. Jung, C., Kim, S., Moon, H. *et al.* Highly Crystalline CVD-grown Multilayer $MoSe_2$ Thin Film Transistor for Fast Photodetector. *Sci Rep* **5**, 15313 (2015). <https://doi.org/10.1038/srep15313>.

9. Lee, H., Ahn, J., Im, S. *et al.* High-Responsivity Multilayer MoSe₂ Phototransistors with Fast Response Time. *Sci Rep* **8**, 11545 (2018). <https://doi.org/10.1038/s41598-018-29942-1>.
10. Chemical Vapor Deposition Growth of Two-Dimensional Compound Materials: Controllability, Material Quality, and Growth Mechanism, Lei Tang, Junyang Tan, Huiyu Nong, Bilu Liu, and Hui-Ming Cheng, *Accounts of Materials Research* **2021** 2 (1), 36-47, DOI: 10.1021/accountsmr.0c00063.
11. Zhu X, Li A, Wu D, et al. Tunable large-area phase reversion in chemical vapor deposited few-layer MoTe₂ films. *J Mater Chem C* 2019; 7:10598–604.
12. J. Li, W. Yan, Y. Lv, J. Leng, D. Zhang, C.O. Coileáin, C.P. Cullen, T. Stimpel-Lindner, G.S., Duesberg, J. Cho, M. Choi, B.S. Chun, Y. Zhao, C. Lv, S.K. Arora, H.C. Wu, Sub-millimeter size high mobility single crystal MoSe₂ monolayers synthesized by NaCl-assisted chemical vapor deposition, *RSC Adv.* 10 (2020) 1580–1587. <https://doi.org/10.1039/c9ra09103c>.
13. Nasrullah Wazir, Ruibin Liu, Chunjie Ding, Xianshuang Wang, Xin Ye, Xie Lingling, Tianqi Lu, Li Wei, and Bingsuo Zou, Vertically Stacked MoSe₂/MoO₂ Nanolayered Photodetectors with Tunable Photoresponses, *ACS Applied Nano Materials* **2020** 3 (8), 7543-7553, DOI: 10.1021/acsanm.0c01195.
14. Zhou, J., Lin, J., Huang, X. *et al.* A library of atomically thin metal chalcogenides. *Nature* **556**, 355–359 (2018). <https://doi.org/10.1038/s41586-018-0008-3>.
15. Nitin T. Shelke, Dattatray J. Late, “Hydrothermal growth of MoSe₂ nanoflowers for photo- and humidity sensor applications”, *Sensors and Actuators A: Physical*, Volume 295, 2019, Pages 160-168, ISSN 0924-4247, <https://doi.org/10.1016/j.sna.2019.05.045>.
16. A Abderrahmane, P J Ko and T V Thu, S Ishizawa, T Takamura, A Sandhu, High photosensitivity few-layered MoSe₂ back-gated field-effect phototransistors, volume 25, 36, *Nanotechnology* IOP Publishing 2014, IOP Publishing, <https://doi.org/10.1088/0957-4484/25/36/365202>.
17. Wang S, Wang G, Yang X, Yang H, Zhu M, Zhang S, Peng G, Li Z., Synthesis of Monolayer MoSe₂ with Controlled Nucleation via Reverse-Flow Chemical Vapor Deposition. *Nanomaterials* (Basel). 2019 Dec 31;10(1):75. doi: 10.3390/nano10010075. PMID: 31906071; PMCID: PMC7023349.

18. Chen, K., Chen, Z. F., Wan, X., Zheng, Z. B., Xie, F. Y., Chen, W. J., Gui, X. H., Chen, H. J., Xie, W. G., Xu, J. B., *Adv. Mater.* 2017, 29, 1700704. <https://doi.org/10.1002/adma.201700704>.
19. Panda, M. R., Gangwar, R., Muthuraj, D., Sau, S., Pandey, D., Banerjee, A., Chakrabarti, A., Sagdeo, A., Weyland, M., Majumder, M., Bao, Q., Mitra, S., High Performance Lithium-Ion Batteries Using Layered 2H-MoTe₂ as Anode. *Small* 2020, 16, 2002669. <https://doi.org/10.1002/sml.202002669>.
20. Manas Ranjan Panda, Anish Raj K, Arnab Ghosh, Ajit Kumar, Divyamahalakshmi Muthuraj, Supriya Sau, Wenzhi Yu, Yupeng Zhang, A.K. Sinha, Matthew Weyland, Qiaoliang Bao, Sagar Mitra, Blocks of molybdenum ditelluride: A high rate anode for sodium-ion battery and full cell prototype study, *Nano Energy*, Volume 64, 2019, 103951, ISSN 2211-2855, <https://doi.org/10.1016/j.nanoen.2019.103951>.
21. Qi, Y., Naumov, P., Ali, M. *et al.* Superconductivity in Weyl semimetal candidate MoTe₂. *Nat Commun* 7, 11038 (2016). <https://doi.org/10.1038/ncomms11038>.
22. Yurii Naidyuk *et al* 2018 *2D Mater.* 5 045014.
23. <https://arxiv.org/abs/2001.01703>.
24. Zhou, L., Xu, K., Zubair, A., Zhang, X., Ouyang, F., Palacios, T., Dresselhaus, M. S., Li, Y., Kong, J., *Adv. Funct. Mater.* 2017, 27, 1603491.
25. Zhou, L., Zubair, A., Wang, Z., Zhang, X., Ouyang, F., Xu, K., Fang, W., Ueno, K., Li, J., Palacios, T., Kong, J. and Dresselhaus, M.S. (2016), Synthesis of High-Quality Large-Area Homogenous 1T' MoTe₂ from Chemical Vapor Deposition. *Adv. Mater.*, 28: 9526-9531. <https://doi.org/10.1002/adma.201602687>.
26. Keum, D., Cho, S., Kim, J. *et al.* Bandgap opening in few-layered monoclinic MoTe₂. *Nature Phys* 11, 482–486 (2015). <https://doi.org/10.1038/nphys3314>.
27. Controlled synthesis and frictional properties of 2D MoTe₂ via chemical vapor deposition, Meng, Lan Xu, Chaoji Li, H. Wang, Xiangfu Yan, *Chemical Physics Letters*, 728, 156-159, 2019.
28. Swee Liang Wong, Chapter 3 - Chemical vapor deposition growth of 2D semiconductors, Editor(s): Dongzhi Chi, K.E. Johnson Goh, Andrew T.S. Wee, In *Materials Today, 2D Semiconductor Materials and Devices*, Elsevier, 2020, Pages 81-101, ISBN 9780128161876, <https://doi.org/10.1016/B978-0-12-816187-6.00003-0>.
29. X. Fan, D.J. Singh, Q. Jiang, W.T. Zheng, Pressure evolution of the potential barriers of phase transition of MoS₂, MoSe₂ and MoTe₂, *Phys. Chem. Chem. Phys.* 18 (2016) 12080–12085, <http://dx.doi.org/10.1039/c6cp00715e>.

30. Huihan Wang *et al* 2018 *Nanotechnology* **29** 314001.
31. Gong, Y., Ye, G., Lei, S., Shi, G., He, Y., Lin, J., Zhang, X., Vajtai, R., Pantelides, S.T., Zhou, W., Li, B. and Ajayan, P.M. (2016), Synthesis of Millimeter-Scale Transition Metal Dichalcogenides Single Crystals. *Adv. Funct. Mater.*, 26: 2009-2015. <https://doi.org/10.1002/adfm.201504633>.

RESEARCH PAPER

Effect of different precursors on morphology of CVD Synthesized MoSe₂

Vinay Kumar Yadav and Vinod Singh*

Department of Applied Physics, Delhi Technological University, Delhi, India-110042

* Corresponding Author, Email: vinodsingh@dtu.ac.in

Abstract

Transition metal dichalcogenides (TMD's) emerged as a very appealing candidate for useful implementations in optoelectronics and electronics devices. In two dimensional TMD's materials, MoSe₂ have a direct bandgap (1.1eV) and possess suitable property for optoelectronics devices. Chemical Vapor Deposition (CVD) represents an attractive approach for the growth of MoSe₂ monolayer and nanoflakes. MoSe₂ is synthesized through CVD method and its structural properties are studied. The variation in morphology was also studied by changing growth temperature and precursor ratio. XRD turned into examine the crystal shape and morphology of a freshly produced MoSe₂ sample and found that the synthesized MoSe₂ nanoflakes crystalline size up to 4-5 μ m without any seeding promoter. We changed the growth temperature and flow rate keeping the pressure constant. As result, a slight change in the crystalline size of MoSe₂ is observed. Further when NaCl is used as a seeding promoter and the pressure is reduced, the crystalline size was reduced and observed to be 0.476 μ m.

KEYWORDS- Transition Metal Dichalcogenides (TMD's) materials, Chemical Vapor Deposition (CVD), 2D materials, Thin film, Nanoflakes, Seeding promoter.

1 Introduction

In this development era, graphene and two-dimensional (2D) substances have emerged as a promising contender for the future electronics because of unique structure, physical property, high carrier mobility, and low resistivity [5]. The non-appearance of the bandgap in graphene has blocked its use in a logic circuit. This non-appearance of bandgap

makes, difficult to control the on/off current in graphene transistors so turning off the graphene-based transistor is a difficult task. This disagreeable property of graphene provoked research on its subordinates and other 2D layered nanomaterials [1]. Transition Metal Dichalcogenides (TMD's) possessing 2D Van Der Waals heterostructure and outstanding properties ranging from insulator to metal. A thin layer of TMD's with equation MX_2 (M= transition metallic of group 4-10, X=S, Se or Te) having properties such as strong spin-orbit coupling, ferromagnetism, quantum spin hall effect, tunable band structure, conventional superconductivity & quantum confinement structure to use for various application in optoelectronics, electronics, energy storage, and photonics [3,5,6,18]. 2D substance exhibit extraordinary light interaction over a bandwidth from infrared to ultraviolet wavelength and permit photodetection on this bandwidth.

MoSe_2 is a kind of layered substance defined through the MX_2 general TMDs formula, where M and X represent Molybdenum (Mo) and Selenium (Se), respectively. The atoms of Mo and Se form a covalent bond and form the Se-Mo-Se basic sheet. MoSe_2 is organized in a sandwich 2D design with interlayer spacing of 6.5\AA by stacking Se-Mo-Se layers on top of each other and connecting them through Van der Waals interaction [4]. Metal selenides, in general, have recently been advised as viable alternatives to usual metal sulphides in order to energy storage [3,6]. In bulk MoSe_2 , the indirect bandgap is 1.1 eV, and throughout monolayer MoSe_2 , the direct bandgap is 1.5 eV [2]. MoSe_2 has a bandgap close to that of Si (1.12 eV), making it suitable for use in optoelectronics and photocatalysts. MoSe_2 has recently acquired a lot of consideration for its potential utilization in electrochemical, photocatalytic, optoelectronic, chemical, and biosensor systems [4,8,9]. Since the vulnerable van der Waals interactions may be overcome to split individual layers of MoSe_2 , much like graphene, this opens up a wide variety of optoelectronic applications, which include light-emitting diodes, light harvesting, optical sensors, and so on [4,9]. MoSe_2 based FET device with carrier mobility ranging from 8 to $38\text{ cm}^2/\text{V}\cdot\text{s}$ and vertically shaped $\text{MoSe}_2/\text{MoO}_2$ heterostructure photodetectors near photoresponsivity of $\sim 100\text{ mA/W}$, the external quantum efficiency of 23.5% at a bias of 3V has been reported [13,16]. For the synthesis, 2D TMDs materials, various methods are available, such as chemical/ mechanical exfoliation, chemical vapor deposition, and Hydrothermal method [3,4,10,11,12,14,17,15]. However, synthesizing monolayer MoSe_2 by Chemical Vapor Deposition (CVD) is still difficult at a large area scale as a result of the low chemical reactivity of Se. Using NaCl like a seeding promoter in the synthesis of MoSe_2 led to

reduced growth time, enhancement of growth rate, and more continuous film production [12,14].

In this work, we used Thermal Chemical Vapor Deposition (CVD) method to synthesize the MoSe₂ thin film samples and nanoflakes. The nanoflakes sample quantity was adequate for satisfactory analysis, so all of the samples have been characterized through X-Ray Diffraction method. Further the structural analysis of the synthesized MoSe₂ nanoflakes is discussed in this article. The ultimate goal is to assess how closely our findings match the standard values of MoSe₂ structural parameters, and thus comment on its morphology evolution with the change of precursor under ambient pressures.

2 Experimental Methods

The whole reaction took place in a split furnace in a 1.3-inch diameter quartz tube. MoSe₂ was obtained by selenization of MoO₃ powder. 10-20 mg MoO₃ powder (99.99% purity, Sigma Aldrich) containing in a ceramic boat located at the center of the furnace, and 0.4-0.5g Se powder (99.99% purity, Sigma Aldrich) in another ceramic boat was located upstream of furnace 12-15cm away from the center. a cleaned 2cm×2cm dimension, 300nm SiO₂/Si substrate placed in MoO₃ containing boat 3-5cm away from the MoO₃ powder towards downstream. A mixture of H₂ and Ar gas flow during the whole reaction, used as carrier gas (5 s.c.c.m. H₂/ 60 s.c.c.m. Ar). The furnace was heated up to 720-880°C with a ramping rate of 14°C/min and kept steady at this temperature for 15 min. After the whole reaction was completed led the furnace cooled right all the way down to room temperature naturally.

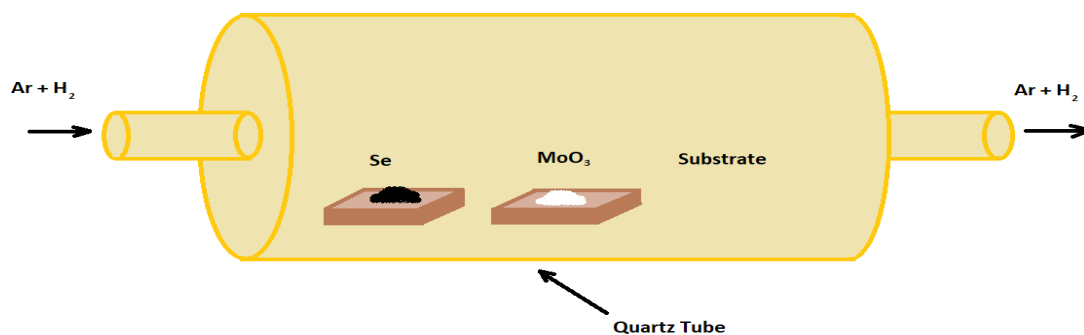


Fig 1: schematic diagram of CVD grown MoSe₂



Fig 2: CVD grown MoSe₂ nanoflakes



Fig 3: CVD grown MoSe₂ thin film on Si/SiO₂ substrate

3 Result and Discussion

The crystal shape and phase evolution of the resulting MoSe₂ sample were confirmed using an X-ray diffractometer. The X-ray diffraction (XRD) characteristic of the resulting MoSe₂ nanoflakes and deposited thin film are shown in Fig 1, 2, 3. Diffraction peaks observed in a scale of 10–80 degrees on the X-ray diffractogram for the MoSe₂ sample. The diffraction peaks detected in the MoSe₂ sample's XRD spectrum reveal a hexagonal crystal shape with growth direction ahead one axis (101). The reported d-spacing values and lattice

variables align well with previous research [JCPDS: 87-2419], which mentioned in below table.

| Sample | Position (2 θ) | Interplanar spacing 'd' (Å) | Crystalline size 'D' (Å) | Lattice parameter |
|--------|--|--|--|--|
| 1) | 13.68 27.46 32.16 41.32 57.83 72.47 | 6.47 3.24 2.78 2.18 1.59 1.30 | 488.56 384.50 514.42 29480.19 513.65 627.01 Avg 5334.72 Å Or 5.33 μm | a=b= 0.277nm & c= 1.29 nm |
| 2) | 13.62 32.15 56.33 69.48 | 6.4 2.78 1.63 1.35 | 4684.27 509.62 11582.65 413.16 Avg- 4297.42Å or 4.3μm | a=b= 0.277nm & c= 1.29nm |
| 3) | 27.53 32.14 59.6 | 3.24 2.78 1.55 | 419.47 434.07 574.59 Avg- 476.04Å or 0.476μm | a=b= 0.277nm & c= 1.29nm |

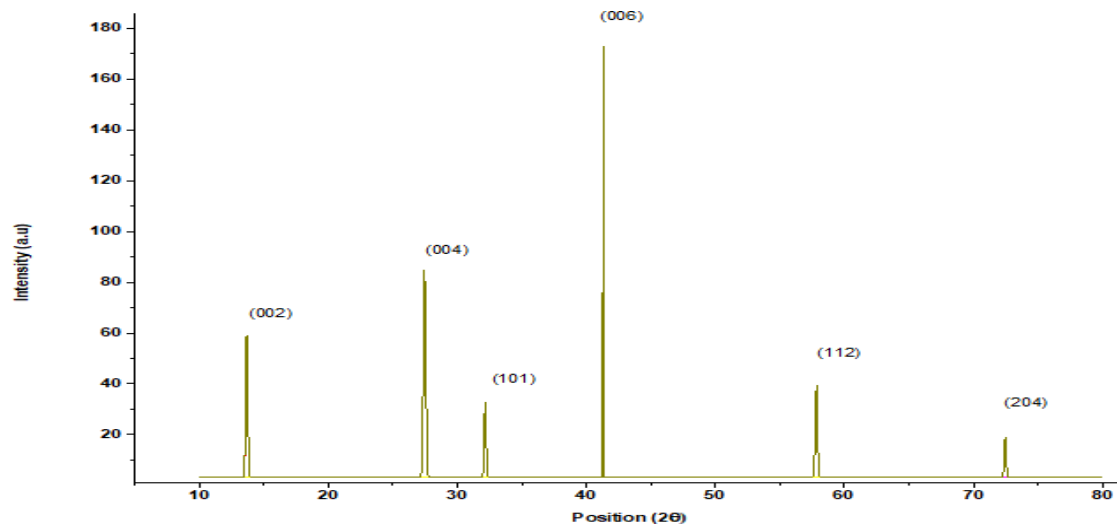


Fig 4: XRD pattern of CVD grown MoSe₂ nanoflakes (growth temperature-725°C, Pressure 760 torr)

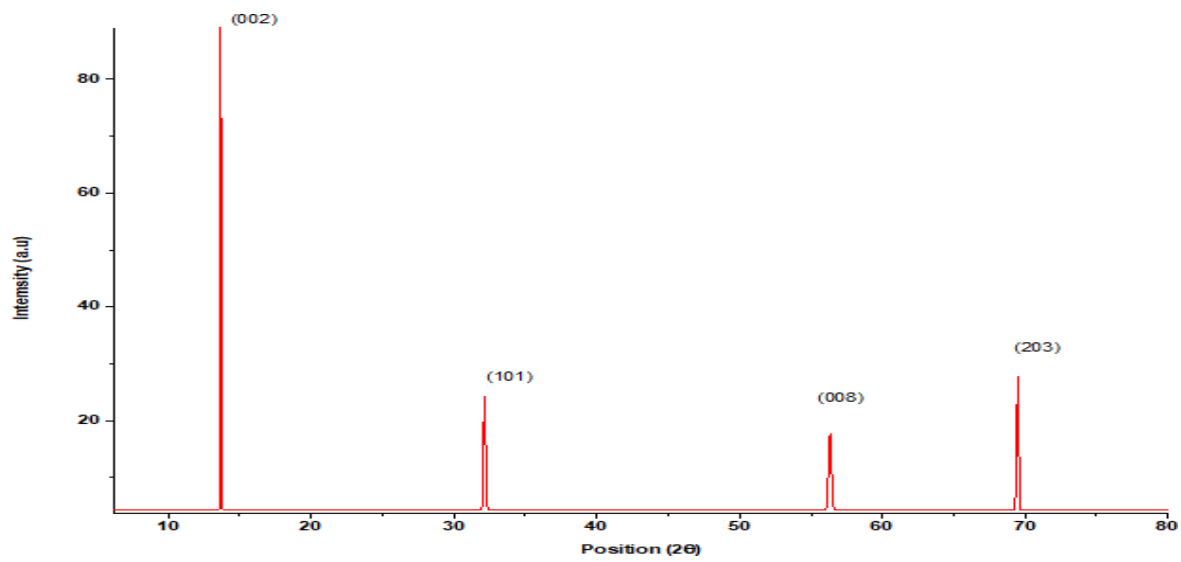


Fig 5: XRD pattern of CVD grown MoSe₂ nanoflakes (growth temperature 820°C, Pressure 760 torr)

In samples 1 and 2 we change the gas flow rate and growth temperature (kept pressure constant 760 torr), from the XRD data we can say that in both samples MoSe₂ nanoflakes formed uniformly with the crystalline size of 5.335 μ m and 4.297 μ m respectively, and doesn't show much crystalline size difference.

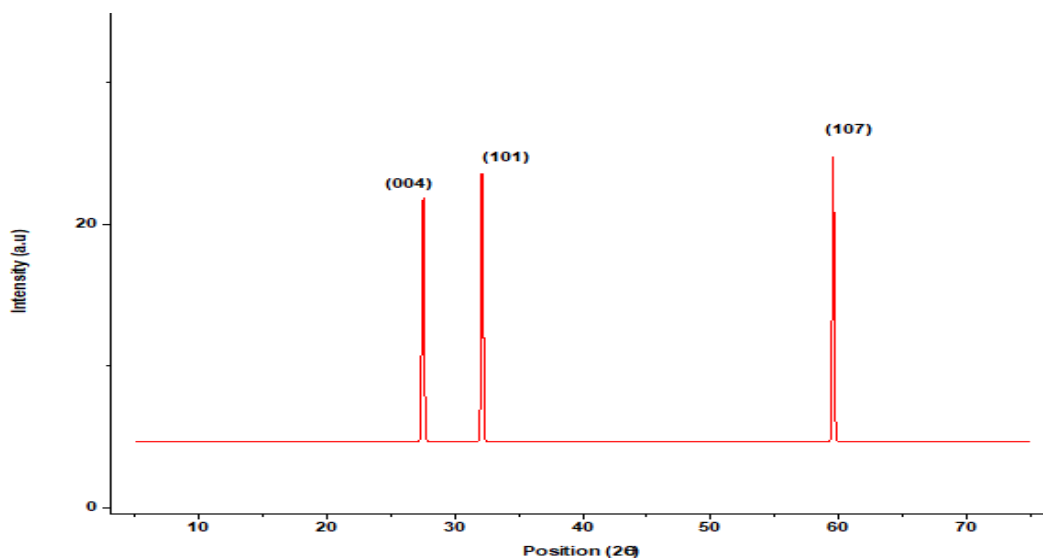


Fig 6: XRD pattern of CVD grown MoSe₂ thin film (Growth temperature 750°C, NaCl as seeding promoter, Pressure 30 torr)

In the same way, when we synthesized NaCl assisted MoSe₂, we reduced the pressure to 30 torr, we found the crystalline size reduced and become 0.476 μ m. here, we were using NaCl as a growth promoter, as it is an oxidizing agent, so reduced the temperature of reaction [12], but it has been observed that there is a major difference of this much in crystalline size.

4 Conclusion

We used Chemical Vapor Deposition (CVD) approach to synthesize a few layers of MoSe₂ nanoflakes. XRD turned into used to analyse the crystal structure and morphology of a freshly produced MoSe₂ sample and found that the synthesized MoSe₂ nanoflakes crystalline size up to 4-5 μ m without any seeding promoter. we change the growth temperature and flow rate but kept the pressure constant. In resultant, there is a slight difference in the crystalline size of MoSe₂. But when we use the seeding promoter (NaCl) kept the same condition but reduced the pressure, the crystalline size was reduced and obtained 0.476 μ m. We conclude that CVD grown MoSe₂ changes with the change of precursor ratio, gas flow rate, growth rate and pressure.

Acknowledgement

The authors would like to extend the deepest gratitude to the Department of Applied Physics, Delhi Technological University for allowing work on this topic. The authors would also like to thank Advanced Instrumentation Lab for XRD, and colleagues from the Nano Fabrication Lab, peer for their constant support and encouragement.

References

1. Kumar, A., Ahluwalia, P.K. Electronic structure of transition metal dichalcogenides monolayers 1H-MX₂ (M = Mo, W; X = S, Se, Te) from ab-initio theory: new direct band gap semiconductors. *Eur. Phys. J. B* **85**, 186 (2012). <https://doi.org/10.1140/epjb/e2012-30070-x>.
2. Sefaattin Tongay, Jian Zhou, Can Ataca, Kelvin Lo, Tyler S. Matthews, Jingbo Li, Jeffrey C. Grossman, and Junqiao Wu, Thermally Driven Crossover from Indirect toward Direct Bandgap in 2D Semiconductors: MoSe₂ versus MoS₂, *Nano Letters* **2012** 12 (11), 5576-5580, DOI: 10.1021/nl302584w.
3. Ali Eftekhari, "Molybdenum diselenide (MoSe₂) for energy storage, catalysis, and optoelectronics", *Applied Materials Today*, Volume 8, 2017, Pages 1-17, ISSN 2352-9407, <https://doi.org/10.1016/j.apmt.2017.01.006>.
4. Fan Jiang, Wen-Sheng Zhao, Jun Zhang, Mini-review: Recent progress in the development of MoSe₂ based chemical sensors and biosensors, *Microelectronic Engineering*, Volume 225, 2020, 111279, ISSN 0167-9317, <https://doi.org/10.1016/j.mee.2020.111279>.
5. Yang L, Xie C, Jin J, Ali RN, Feng C, Liu P, Xiang B. Properties, Preparation and Applications of Low Dimensional Transition Metal Dichalcogenides. *Nanomaterials* (Basel). 2018 Jun 26;8(7):463. doi: 10.3390/nano8070463. PMID: 29949877; PMCID: PMC6071048.
6. Manas Ranjan Panda, Anish Raj K, Arnab Ghosh, Ajit Kumar, Divyamahalakshmi Muthuraj, Supriya Sau, Wenzhi Yu, Yupeng Zhang, A.K. Sinha, Matthew Weyland, Qiaoliang Bao, Sagar Mitra, Blocks of molybdenum ditelluride: A high rate anode for sodium-ion battery and full cell prototype study, *Nano Energy*, Volume 64, 2019, 103951, ISSN 2211-2855, <https://doi.org/10.1016/j.nanoen.2019.103951>.
7. [Titao Li](#), [Zhaojun Zhang](#), [Wei Zheng](#), [Yangyang Lv](#), and [Feng Huang](#), "A possible high-mobility signal in bulk MoTe₂: Temperature independent weak phonon decay", *AIP Advances* 6, 115207 (2016) <https://doi.org/10.1063/1.4967351>.
8. Jung, C., Kim, S., Moon, H. *et al.* Highly Crystalline CVD-grown Multilayer MoSe₂ Thin Film Transistor for Fast Photodetector. *Sci Rep* **5**, 15313 (2015). <https://doi.org/10.1038/srep15313>.
9. Lee, H., Ahn, J., Im, S. *et al.* High-Responsivity Multilayer MoSe₂ Phototransistors with Fast Response Time. *Sci Rep* **8**, 11545 (2018). <https://doi.org/10.1038/s41598-018-29942-1>.

10. Chemical Vapor Deposition Growth of Two-Dimensional Compound Materials: Controllability, Material Quality, and Growth Mechanism, Lei Tang, Junyang Tan, Huiyu Nong, Bilu Liu, and Hui-Ming Cheng, *Accounts of Materials Research* **2021** 2 (1), 36-47, DOI: 10.1021/accountsmr.0c00063.
11. Zhu X, Li A, Wu D, et al. Tunable large-area phase reversion in chemical vapor deposited few-layer MoTe₂ films. *J Mater Chem C* 2019; 7:10598–604.
12. J. Li, W. Yan, Y. Lv, J. Leng, D. Zhang, C.O. Coileain, C.P. Cullen, T. Stimpel-Lindner, G.S., Duesberg, J. Cho, M. Choi, B.S. Chun, Y. Zhao, C. Lv, S.K. Arora, H.C. Wu, Sub-millimeter size high mobility single crystal MoSe₂ monolayers synthesized by NaCl-assisted chemical vapor deposition, *RSC Adv.* 10 (2020) 1580–1587. <https://doi.org/10.1039/c9ra09103c>.
13. Nasrullah Wazir, Ruibin Liu, Chunjie Ding, Xianshuang Wang, Xin Ye, Xie Lingling, Tianqi Lu, Li Wei, and Bingsuo Zou, Vertically Stacked MoSe₂/MoO₂ Nanolayered Photodetectors with Tunable Photoresponses, *ACS Applied Nano Materials* **2020** 3 (8), 7543-7553, DOI: 10.1021/acsnm.0c01195.
14. Zhou, J., Lin, J., Huang, X. *et al.* A library of atomically thin metal chalcogenides. *Nature* **556**, 355–359 (2018). <https://doi.org/10.1038/s41586-018-0008-3>.
15. Nitin T. Shelke, Dattatray J. Late, “Hydrothermal growth of MoSe₂ nanoflowers for photo- and humidity sensor applications”, *Sensors and Actuators A: Physical*, Volume 295, 2019, Pages 160-168, ISSN 0924-4247, <https://doi.org/10.1016/j.sna.2019.05.045>.
16. A Abderrahmane, P J Ko and T V Thu, S Ishizawa, T Takamura, A Sandhu, High photosensitivity few-layered MoSe₂ back-gated field-effect phototransistors, volume 25, 36, *Nanotechnology* IOP Publishing 2014, IOP Publishing, <https://doi.org/10.1088/0957-4484/25/36/365202>.
17. Wang S, Wang G, Yang X, Yang H, Zhu M, Zhang S, Peng G, Li Z., Synthesis of Monolayer MoSe₂ with Controlled Nucleation via Reverse-Flow Chemical Vapor Deposition. *Nanomaterials* (Basel). 2019 Dec 31;10(1):75. doi: 10.3390/nano10010075. PMID: 31906071; PMCID: PMC7023349.
18. Chen, K., Chen, Z. F., Wan, X., Zheng, Z. B., Xie, F. Y., Chen, W. J., Gui, X. H., Chen, H. J., Xie, W. G., Xu, J. B., *Adv. Mater.* 2017, 29, 1700704. <https://doi.org/10.1002/adma.201700704>.